Contents

Introduction

I took part to the Summer School organized by Fermilab and Università degli Studi di Pisa, working on site from 1st August to 30th September 2022. I have worked with DUNE collaboration, with Falvio Cavanna and Alexander Kish as supervisors. The task assigned to me was the following:

"""Development of the photon detection system for DUNE Vertical Drift TPC.

The design of the Far Detector 2 of the Deep Underground Experiment (DUNE) is based on innovative vertical drift liquid argon time-projection chamber (TPC), which will be instrumented with large-area photodetection modules to search for neutrino interactions with low energy deposits via scintillation signal. The photosensors will be operating in cryogenic environment and in high electric field. All electric power and signal will be transmitted via optical fiber guides.

Fermilab is leading the development of the power delivery over fiber (PoF) and front-end electronics for analog and digital optical signal transmission (SoF). Dedicated R&D and test facility is in operation at the FNAL Proton Assembly Building (PAB).

The activities foreseen for the period of August-September are: characterization of silicon photomultipliers (SiPMs) and their aggregated read-out, optimization of the analog optical readout electronics and SoF, studies with PoF, down-selection of the bias voltage generation solutions, laser diodes and their assemblies, optical fibers and connectors.

Summer student will participate in all activities related to the project, from planning the test and qualification procedures to their implementation, preparation of test stands, measurements involving thermal cycling in cryogenic liquids (argon and nitrogen), data acquisition, its analysis and interpretation, and preparation of technical notes and reports."""

In this Final Term Report, I will explain the core of my work at FNAL and future plans.

Chapter 1

DUNE

1.1 Overview

The term **DUNE** stands for "**Deep Underground Neutrino Experiment**". The program will be carried out as an international, leading-edge, dual-site experiment for neutrino physics and proton decay studies, indeed, the main objective of this experiment is to study long-baseline neutrino oscillations (fig. 1.1)(experiments carried out over the past half century have revealed that neutrinos are found in three states, or *flavors*, and can transform from one flavor into another. These results indicate that each neutrino flavor state is a mixture of three different nonzero mass states). Moreover, this studies will help us discover more about why matter is more abundant than antimatter (the so called *matter-antimatter asymmetry*) and DUNE's capability to collect and analyze neutrino signal from a supernova within the Milky Way would provide a rare opportunity to peer inside a newly formed neutron star and potentially witness the birth of a Black Hole.

Figure 1.1: Neutrino oscillations.

1.2 The experiment

To achieve its goals, the international DUNE experiment, hosted by the U.S. Department of Energy's Fermi National Accelerator Laboratory (Fermilab) in Illinois, comprises three main components (fig. 1.2):

1) a **Long-Baseline Neutrino Facility (LBNF)**, hosted by Fermilab, that will deliver the world's highest-intensity neutrino beam, generated from a proton accelerator at Fermilab;

2) a high-precision **Near Detector (ND)** on the Fermilab site able to characterize and monitor the beam;

3) a massive **Far Detector (FD)** installed deep underground at the Sanford Underground Research Facility (SURF) 1300 km away in Lead, South Dakota.

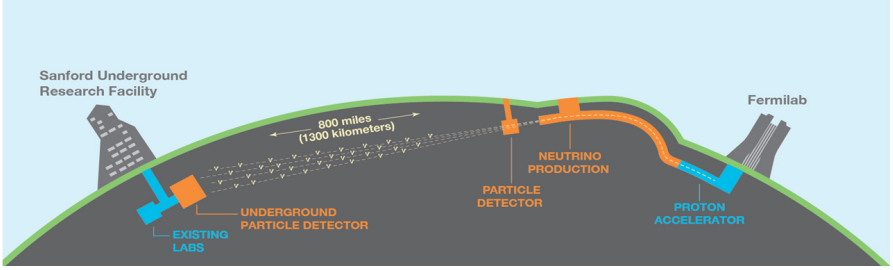

Figure 1.2: Configuration of the LBNF beamline at Fermilab, in Illinois, and the DUNE Near and Far Detectors in Illinois and South Dakota, separated by 1300 km.

1.2.1 Far Detector

The Far Detector will be the largest and most technologically advanced liquid-argon neutrino detector, composed of 4 massive liquid argon time-projection chambers (LArTPCs), installed approximately 1.5 km underground. Each LArTPC will be hosted by a cryostat of internal dimensions 15.1 m (w) × 14.0 m (h) × 62.0 m (l) containing a LAr mass of about 17.5 kt, for a total of nearly 70kt.

DUNE is planning for and currently developing two LArTPC technologies: single-phase (SP) in which all the detector elements inside the cryostat are immersed in liquid; and dual-phase (DP), in which some components operate in a layer of gaseous argon above the liquid:

- in the SP technology, ionization charges drift horizontally (**HD-LArTPC**) in LAr under the influence of an electric field (E field) towards a vertical anode, where they are read out.
- in the DP technology (fig. 1.3), ionization charges drift vertically (**VD-LArTPC**) in LAr and are transferred into a layer of argon gas above the liquid, and devices called Large Electron Multipliers (LEMs) amplify the signal charges in the gas phase before they reach a horizontal anode.

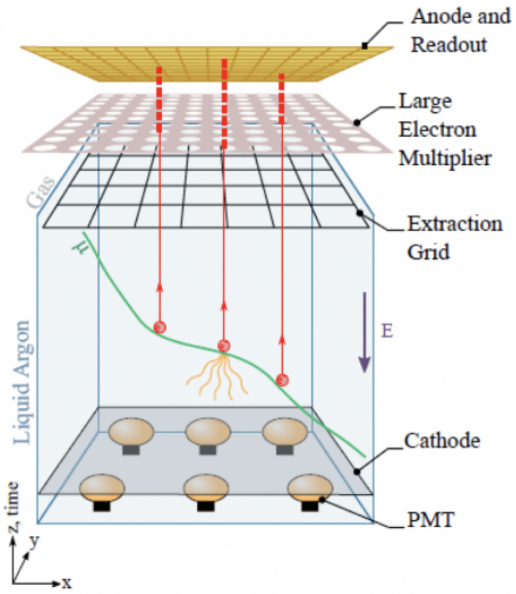

Figure 1.3: The general operating principle of the DP LArTPC.

In both technologies, the drift volumes are surrounded by a field cage (FC) that defines the active detector volume and ensures uniformity of the E field within that volume.

1.2.2 VD-LArTPC

In the VD design (fig. 1.4), charge generated by ionization is drifted towards a set of grids which allows the reconstruction of particles' trajectories inside the chamber. Argon scintillation light is also collected providing fast timing information used in event time reconstruction, precise calorimetric energy reconstruction, efficient triggering capability, and to reduce energy threshold and study low-energy neutrino interactions (i.e. SuperNova neutrinos).

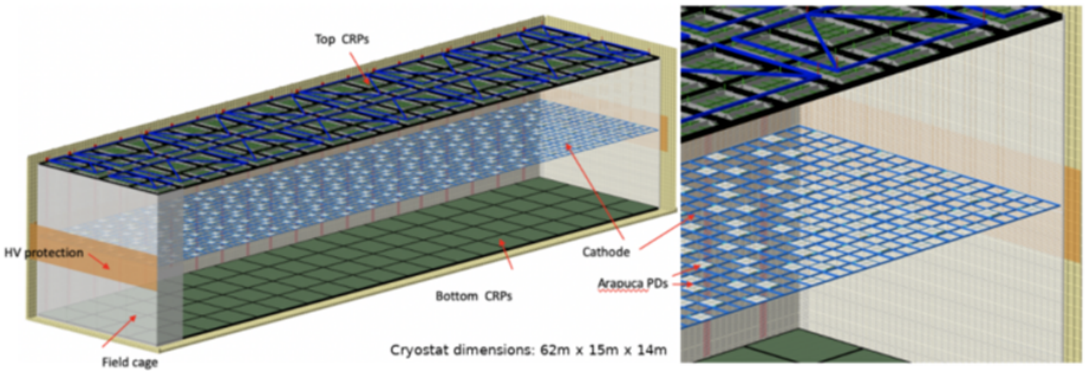

Figure 1.4: VD LArTPC.

1.3 LAr technology

Argon is an excellent scintillator at a wavelength of 127 nm (UV), a property that both detector designs exploit. This fast scintillation light (photons), once shifted into the visible spectrum, is collected by photon detectors (PDs) in both designs. The light collection provides an initial start time (t_0) for every event recorded by the time projection chamber (TPC), indicating when the ionization electrons begin to drift. Comparing the time at which the ionization signal reaches the anode relative to this start time allows reconstruction of the event topology in the drift coordinate (i.e. horizontal and transverse to the beam for SP and vertical for DP).

With an average energy of 19.5 eV needed to produce a photon (at zero field), a typical particle depositing 1 MeV in LAr will generate 40,000 photons with wavelength of 128 nm. At higher fields this will be reduced, but at 500 V/cm the yield is still around 20,000 photons per MeV. Roughly 1/4 of the photons are promptly emitted with a lifetime of about 6 ns while the rest havea lifetime of 1100–1600 ns. Prompt and delayed photons are detected in precisely the same way by the photon detection system. The relatively large light yield makes the scintillation process an excellent candidate for determination of t_0 for non-beam related events.

Two key factors affect the performance of the DUNE LArTPCs: LAr purity (high to minimize charge and light attenuation over the longest drift lengths in the detector module) and noise on the cryogenic readout electronics.

1.3.1 Photon Detection System

The **Photon Detection System (PDS)** will use large $60 \times 60 cm^2$ *X-Arapucas* (fig. 1.5), a box with highly reflective internal walls and with a set of wavelength shifters and a dichroic

filter designed to trap photons on the inside of the device so they can be detected by silicon photomultipliers (SiPMs).

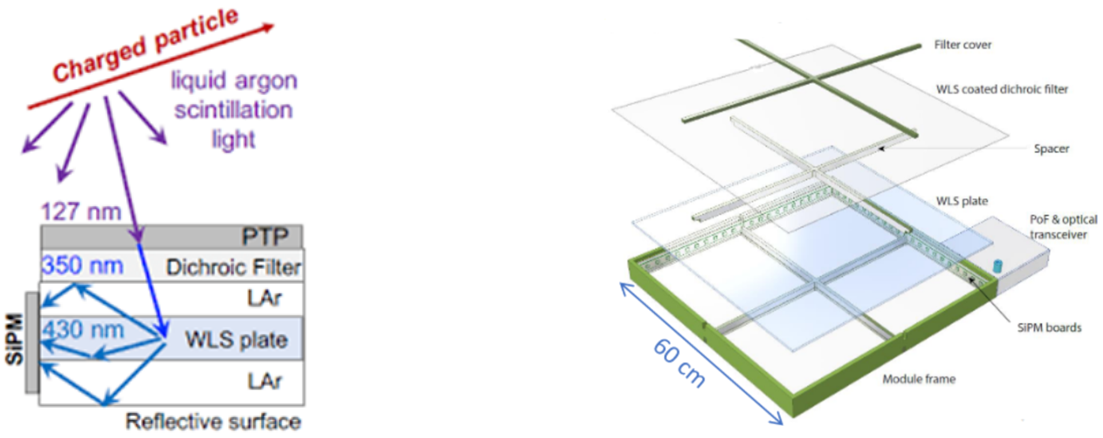

(a) (b)

Figure 1.5: An "arapuca" is a South American bird trap; the name is used here as an analogy to the way the devices trap photons. These devices have been developed by DUNE collaborators in Brazil.

1.4 Power supply and signal readout

1.4.1 Power and Signal over Fiber

Power will be supplied over fiber, indeed, the light of a high-power laser will be transmitted using multi-mode fibers to a photovoltaic power converter placed inside the cryostat and close to the photo-sensors. The readout will be made through optical fiber as well, using an Analog Optical Transmitter inside the cryostat to transform the analog signal produced by PDs into an optical signal and bring this to an Optical Receiver, which converts this optical signal into an analogical one, ready to be acquired by an ADC (both the Receiver and the Digitizer will be placed in warm - fig. 1.6). Fermilab is leading the development of the **Power Delivery Over Fiber (PoF)** and front-end electronics for **Analog and Digital Optical Signal Transmission (SoF)**. Dedicated R&D and test facility is in operation at the FNAL Proton Assembly Building (PAB).

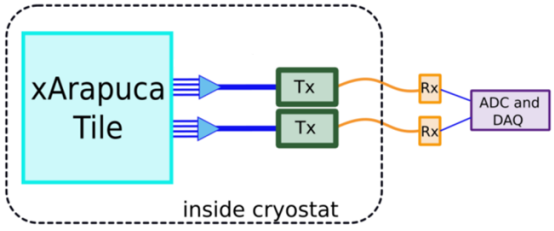

Figure 1.6: Scheme of Signal over Fiber transmission: Tx is the Analog Optical Transmitter while Rx is the Optical Receiver).

Chapter 2

My Work at FNAL

The main aim of my work at FNAL is to test and characterize silicon photomultipliers (SiPMs) and their aggregated read-out, together with the optimization of the analog optical readout electronics (SoF). Firstly, I was engaged into the assembly of the experimental setup required to complete such a task, so I was able, helped by my supervisors, to learn about and test all the electrical and optical components involved. After we have ensured that the setup was able to take data, we took some runs with the digitizer and the analysis part of my work could start. In this section, I will show the hardware side of the work, trying to explain how the experiment was setted up and how all the several components work.

2.1 Experimental Setup

Starting from bottom left of fig. 2.1, there is a 20 SiPMs test card (Hamamatsu, S14160/S14161 series), which was put in a Liquid Argon bath and illuminated by light diffused by a diffuser and produced by an LED. This test card has 3 connectors: (i) Bias (green cable, indicated with letter B), which supplies the necessary voltage given by a voltage supplier, that in this case I set to give 36V, i.e. above the breakdown voltage of the SiPMs in LAr (which is around 32V); (ii) Cathode (black cable, indicated with letter C) and (iii) Anode (red cable, indicated with letter A), which are the output and are connected to che following component, that is the Analog Optical Transmitter, and I used an Argon 2x2 Board 8 (5V voltage supplied) of the DUNE Collaboration. In this case, I used the AC channel, since the DC one was not functioning. This board is able to amplify the signal coming from the SiPMs, converts it into an optical signal and then transmits it through an Optical Fiber (Single Mode, $9\mu m$ diameter, yellow fiber in the picture) to the Optical Receiver, in this case I used a Koheron PD100 (connected to a voltage supplier which supplies $\pm 7V$ and the Ground). The Koheron is able to convert the optical signal in input into an analog signal ready to be acquired by an ADC (CAEN Mod. V1720, 8 channels, 12 bits, TTL Logic), using the LED as Trigger.

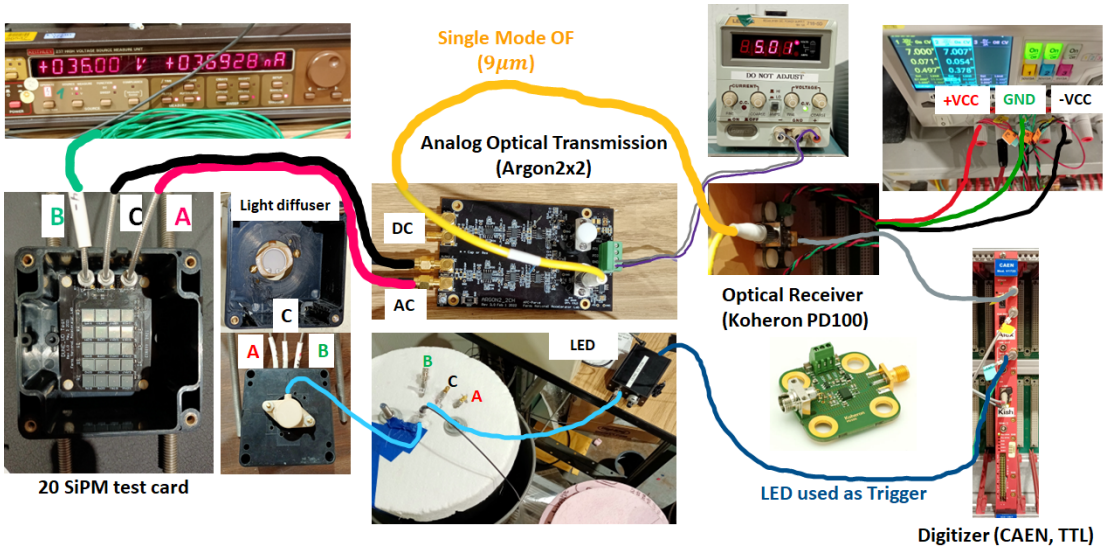

Figure 2.1: Experimental Setup.

In a second phase of characterization and testing, two elements have been changed (fig. 2.2):

1. the SiPM board produced by Hamamatsu has been changed with one arrived from Broadcom (AFBR-S4N66P024M), which has a lower breakdown voltage in LAr, around 28V;

2. the Analog Optical Transmitter, from the *Argon 2x2 Board* to *Argon SimpX3*.

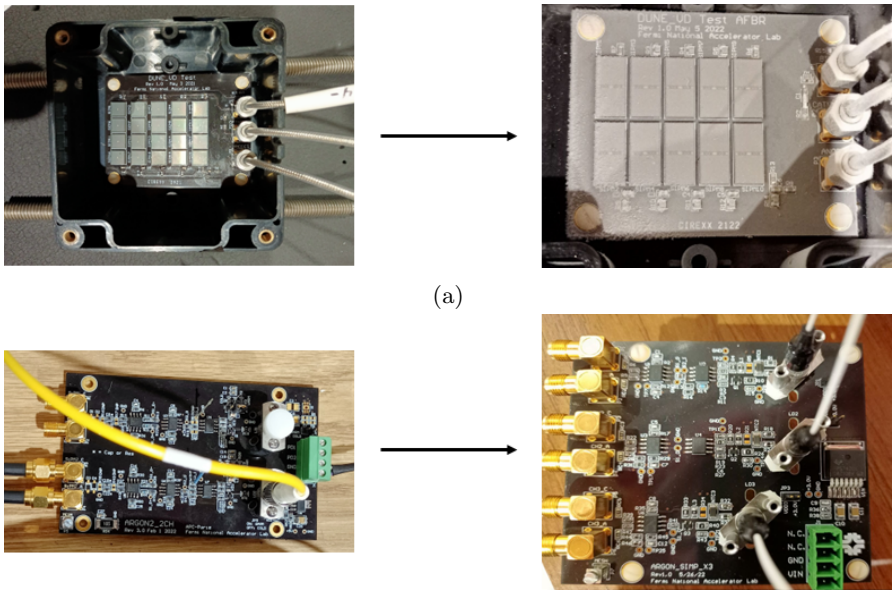

(a)

(b)

Figure 2.2: On the left, SiPM board (top) and Analog Readout (Bottom) used in the first setup, while on the right there are their implementation

2.2 Photo-detectors

2.2.1 SiPM

A SiPM is a matrix made of base elements called SPADs (*Single Photon Avalanche Diodes*, fig. 2.3). These are semiconductor based devices which operates in Geiger mode and are able to produce a high current in response to the arrive of a photon, however, this current can saturate, making the device not sensitive to new incoming radiation. For this reason, a "quenching" resistor is placed in series. All the SPADs are in parallel, so their current is summed, which means that, since the current produced by each of them is fixed to the one produced for one photon detected, this device can count how many photons impact its surface.

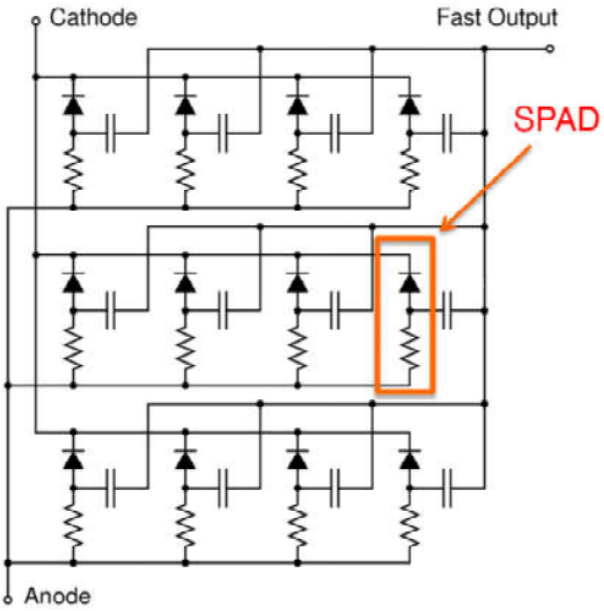

Figure 2.3: SiPM principle of functioning.

2.3 Optical Readout

2.3.1 Analog Optical Transmission

DUNE VD will have a system which can convert an analog signal, e.g. coming from the SiPMs of the photon detection system (PDS), into an optical one that can be transmitted through optical fiber. Such a device works based on a simple element: a laser diode. A laser diode is a semiconductor device similar to a light-emitting diode (LED) in which a diode pumped directly with electrical current can create lasing conditions at the diode's junction. Driven by voltage, the doped p–n-transition allows for recombination of an electron with a hole. Due to the drop of the electron from a higher energy level to a lower one, radiation, in the form of an emitted photon is generated. This is spontaneous emission. Stimulated emission can be produced when the process is continued and further generates light with the same phase, coherence and wavelength. In order to achieve this condition, several stages of amplification are used to amplify the signal coming from the SiPM board.

We used two different boards as analog readout:

1. Argon_2x2_Board, for data taken on 1 September 2022 (fig. 2.4a);

2. Argon_Simp_X3, for data taken on 20 September 2022 (fig. 2.4b);

Schematic for both SiPMs board can be found in the Appendix, as well as for Argon SimpX3.

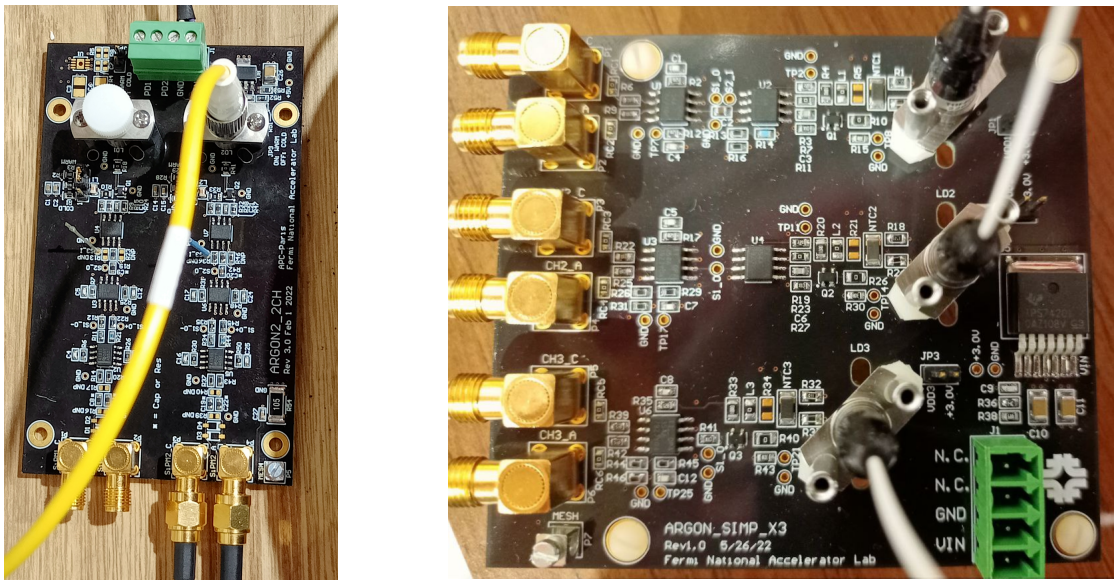

(a) (b)

Figure 2.4: Argon_2x2_Board on the left, Argon_Simp_X3 on the right.

2.3.2 Optical Receiver

The optical receiver is a device used to convert the optical signal coming from the analog readout (Argon_2x2_Board or Argon_Simp_X3 in my case) into an analog signal ready to be acquired by an ADC. The one used in my setup is the *Koheron PD100* (fig. 2.5).

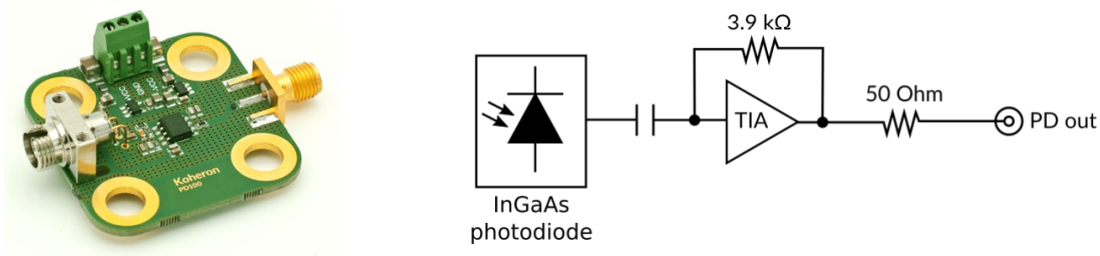

(a) (b)

Figure 2.5: On the left, there is an image of the Koheron PD100, while on the right its schematic.

Chapter 3

Data Analysis

The aim of data analysis is to develop a code that is able to completely characterize SiPMs used in the experiment. This code should determine important properties of these boards (like Gain, Signal to Noise Ratio and Resolution to Single Photoelectron), in order to select the best configuration of SiPMs and Optical Transmitter to use. Moreover, this code, once finally developed and approved, could be used in the normal characterization routines at PAB (Proton Assembly Laboratory, located in Fermilab).

Data shown in the following analysis have been taken in PAB on 1 September 2022 or on 20 September 2022. On the first date, We used only Hamamatsu SiPM board with Argon 22x2 Board as analog readout, while on the second date we tried both Hamamatsu and Broadcom boards with the new analog readout. The main purpose of the analysis has been to develop the code necessary to characterize a SiPM response to LED flashes and to test several devices and components (as I have already mentioned), in order to give a feedback on their performances.

3.1 Data taken on 1st September 2022

3.1.1 Waveform Example

The data file I took containes 10k events (i.e. 10k waveforms), and each of them has 5000 samples, for a total time length of $20\mu s$ per event (sampling rate of 0.25 GHz). I have calculated the baseline for each event and filter applied and then subtracted it to each point. The baseline value to subtract, let's say μ_{bsl}, has been calculated as the mean value of the voltage in the first 300 samples ($1.2\mu s$ from the start, colored in yellow in fig. 3.1) for each waveform and filter separately. The dashed lines represent the values of amplitudes corresponding to $\pm 3\sigma_{bsl}$, where σ_{bsl} is the standard deviation of the distribution of the amplitude values in the same first 300 samples, and represents the dispersion of these 300 points around the mean value of the baseline. In fig. 3.1, there is an example of waveform taken with the setup shown in the previous chapter. On the top left, we can see the raw waveform while the other 3 quarters of image are obtained applying 3 different digital filters to raw data, in order to suppress high frequency noise, in order: Median (top right), Gaussian (bottom left) and Savitzky-Golay (bottom right).

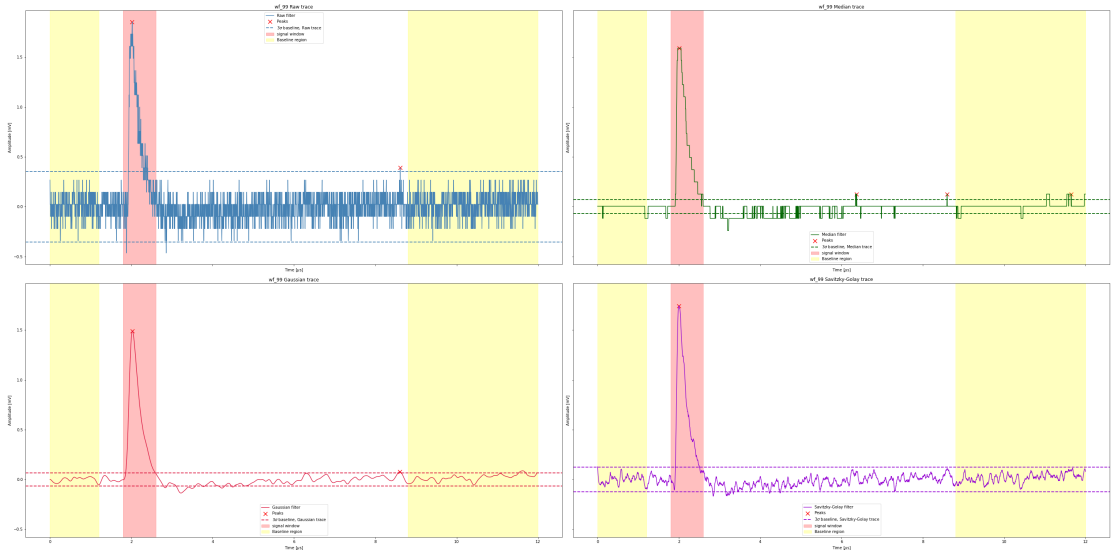

Figure 3.1: Example of raw and with filters applied waveforms. In order: Raw (top left), Median (top right), Gaussian (bottom left), Savitzky-Golay (bottom right). Data taken on: 1 September 2022.

Moreover, the baseline regions (represented by the area between the two dashed lines in fig. 3.1) change with the kind of filter applied: raw waveform, since there is no filter applied to remove noise, has the widest baseline region, while it gets narrower applying a filter. Generally speaking, I have noticed that applying Gaussian filter gives a smaller baseline dispersion with respect to Savitzky-Golay filter (both smaller than Raw data in fact), while Median filter results in a non-constant effect to the baseline region.

Finding Peaks

In my analysis, I have implemented an algorithm that is able to find peaks in an event (based on some characteristics of these peaks), retrieve their main parameters (such as width, height, prominence, sample and time at which it is recorded) and calculate the optimal window where to integrate the main peak and calculate the charge associated with it (shown in red in fig. 3.1). The window can be set as fixed or determined in the following way: the starting and ending samples of the integration window are selected as those samples for which the voltage values are respectively the first and the last above a certain threshold *thr* (in my case, I used $thr = 3\sigma_{bsl}$, so that it is possible avoid noise).

3.1.2 Mean Baseline Distribution

Once I have calculated the baseline averages for each event and filter, I could just plot these values (filter by filter) and fit these distributions with a gaussian (fig. 3.2), in order to calculate a mean and an error associated with it.

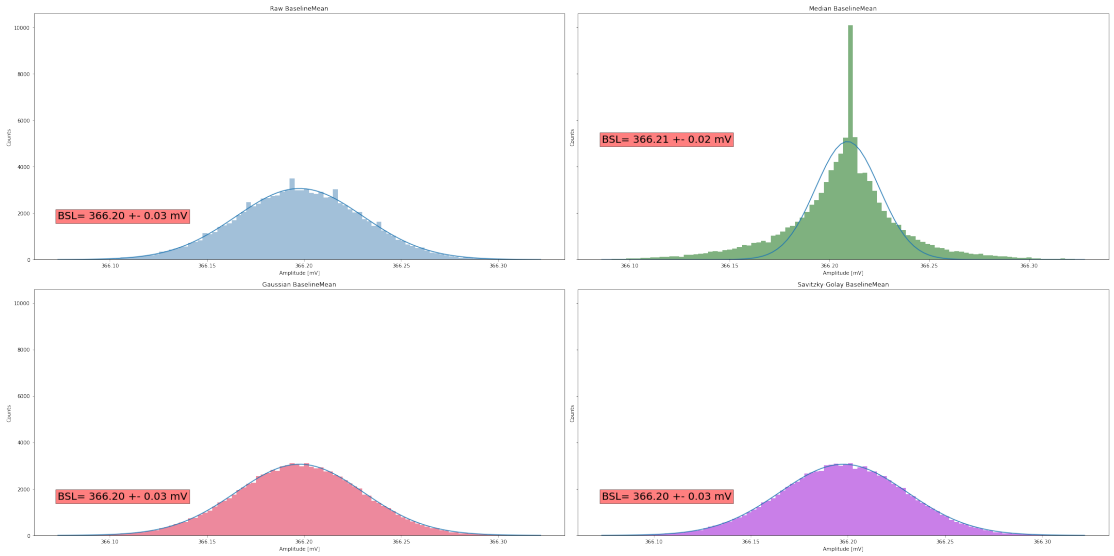

Figure 3.2: Distributions of baseline averages for all events and filters applied. Notice that the mean is the same within errors.

As shown, all values obtained are comparable within errors, so applying a filter does not change the mean value of the average of the baselines computed on all events, but just the dispersion (in particular, they tend to reduce it as shown in fig. 3.1) of baseline samples (for instance, the first 300 ones) around this mean value.

3.1.3 Finger Plot

The main properties used in the following analysis are peaks' amplitudes and charges, that help us create the so called **Finger Plot** (the name comes from the characteristic peaks which should arise).

Using Amplitudes

For each event (waveform) we consider the amplitudes of all peaks found, and make an histogram across all the events. What we obtained with this dataset is shown in fig. 3.3.

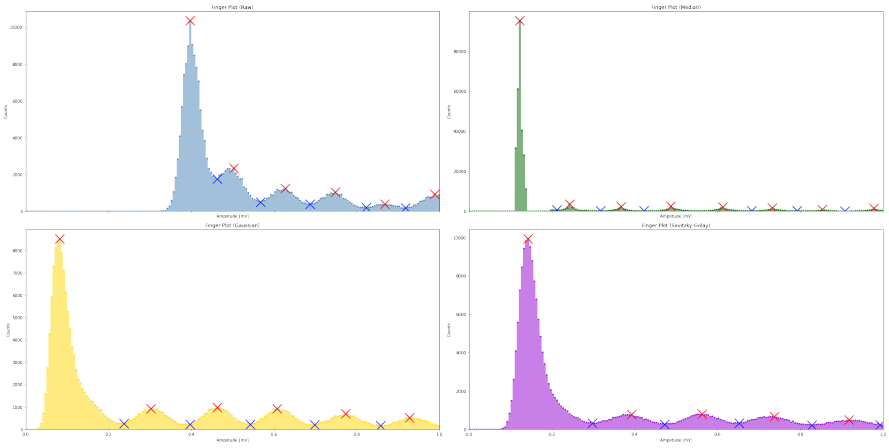

(a)

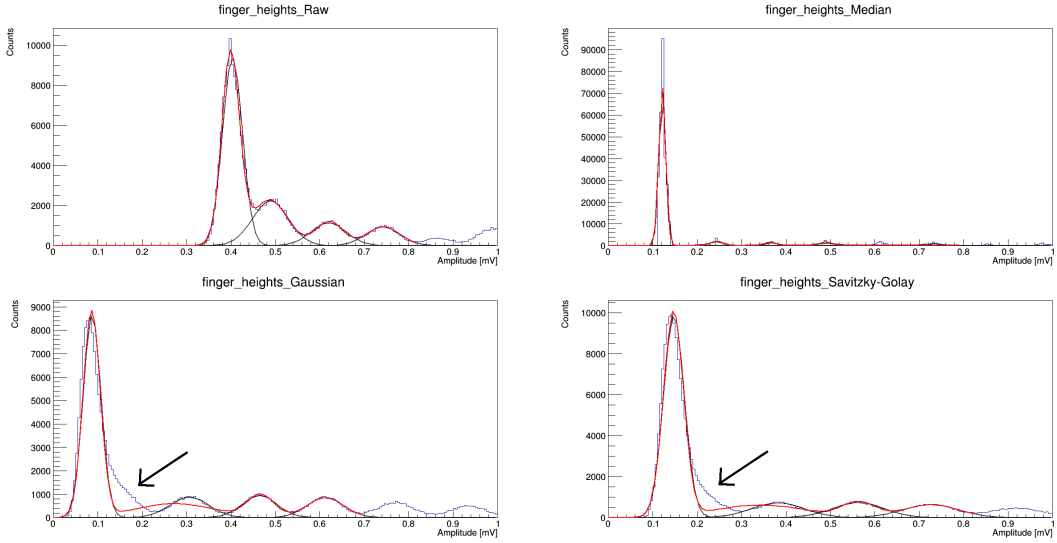

(b)

Figure 3.3: Finger Plot with peaks' amplitudes.

In fig. 3.3a, we can see how the algorithm is able to find peaks and minima in order to autoset the ranges to fit the several peaks, while in fig. 3.3b we have the partial and total fits performed. For some of the filters (in this case Gaussian and Savitzky-Golay) there are some problems with the fit, messed up by some events indicated with a black arrow. These events can be noise (should be possible to remove applying some cuts on peaks properties, and this would be a future improvement of the code), or the superimposition of the first two peaks (maybe pedestal and SPE but not validated) due two low resolution of the system. Plotting the means of the peaks obtained with the fit against the number of the peak, we can obtain fig. 3.4.

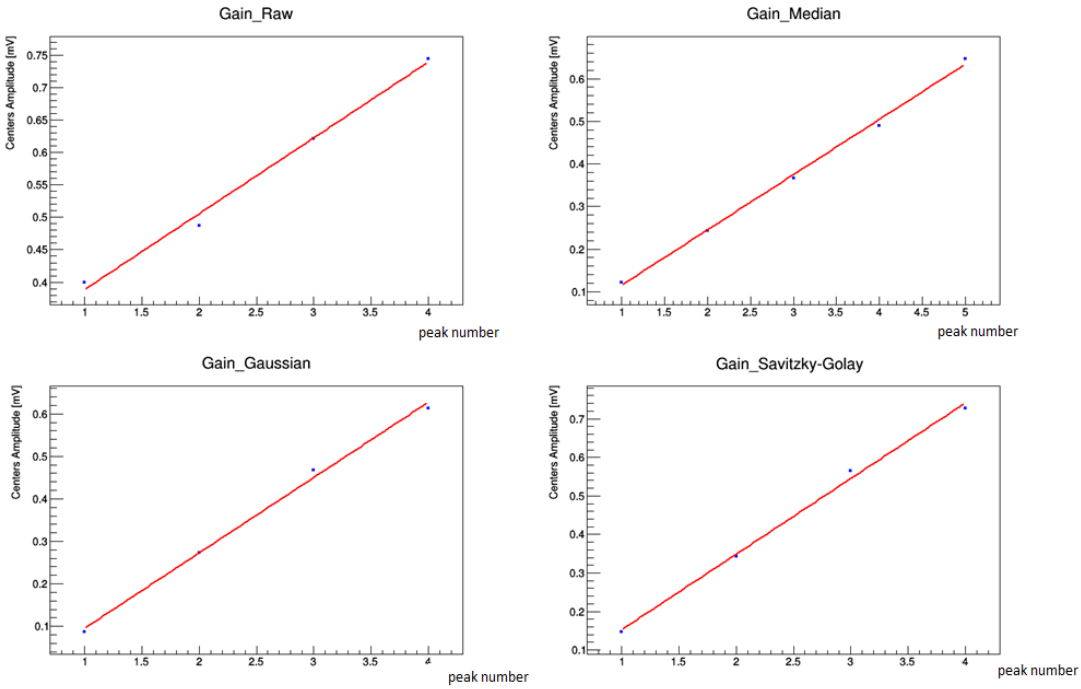

Figure 3.4: Gain_Amplitudes_1.

We can observe the expected linear behaviour, but we can't validate data, since it is still not possible to determine if the first peak representes the Pedestal or 1 or more p.e.. Further analysis and improvements in the code should let us undertsand something more.

Using Charges

For each event (waveform) we consider the amplitudes of all peaks found, and make a histogram across all the events. What we obtained with this dataset is shown in fig. 3.5.

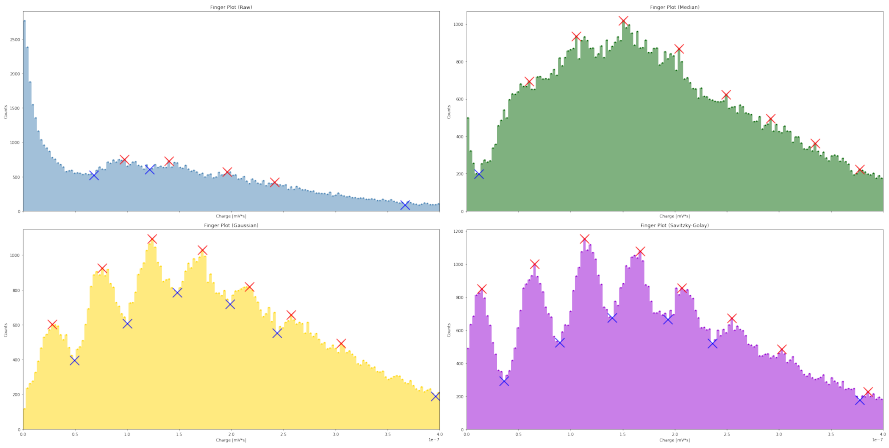

(a)

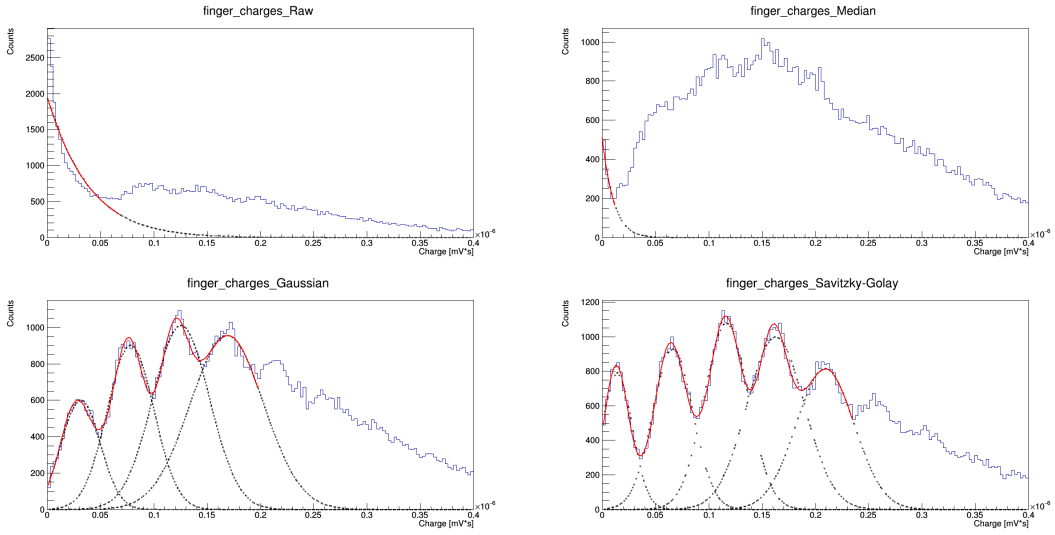

(b)

Figure 3.5: Finger Plot with peaks' amplitudes.

In this case, we have no resolution with Raw Data and Median filter, while some peaks arise using Gaussian or Savitzky-Golay filters. Plotting the means against the peak number, I obtain fig. 3.6 but get the same uncertainty problems arisen with amplitudes analysis.

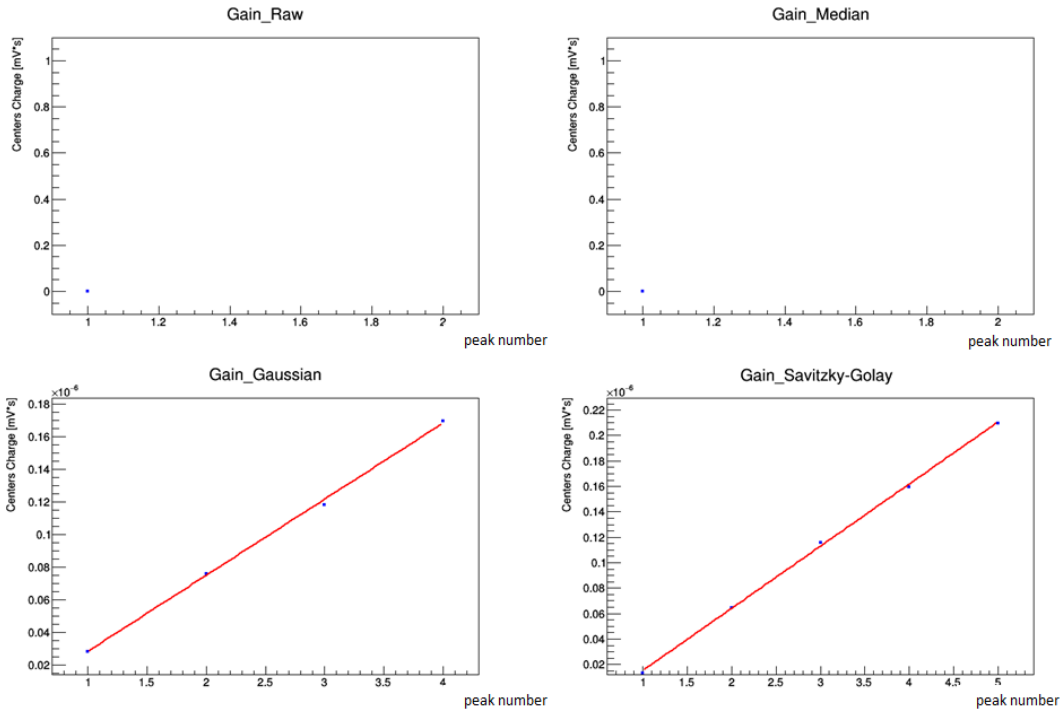

Figure 3.6: Gain_Charges_1.

3.2 Data taken on 20th September 2022

In this data acquisition, we swapped the Argon_2x2 Board with the new designed one, the Argon_SIMP_X3, and used both SiPM Boards (Hamamatsu and Broadcom), in order to test the new components.

3.2.1 Waveform Example

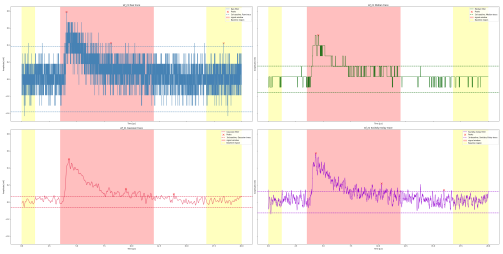

(a) Run 1608. Broadcom, 7.0, 40V.

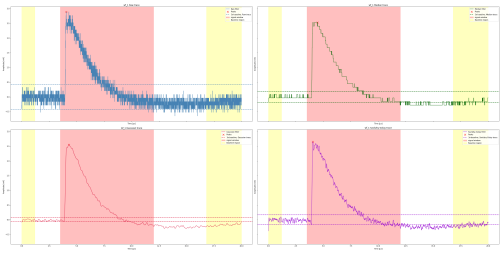

(b) Run 1553. Broadcom, 10.0, 40V.

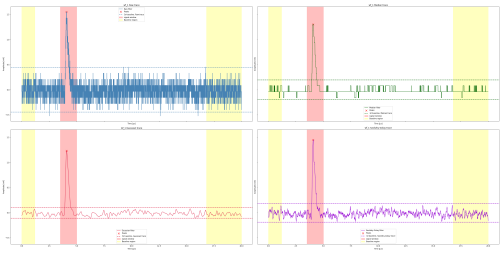

(c) Run 1638. Hamamatsu, 6.4, 38V.

Figure 3.7: Waveform examples coming from three different datasets. Type of SiPM, LED intensity and Bias voltage used are reported for each of them.

As we can see from fig. 3.7 Broadcom SiPM board has longer pulses and higher undershoot with respect to Hamamatsu one, making the system not sensitive and able to detect new photons for longer time. For this reason, we want to avoid these two problems. From now on, data coming from run 1553 will be shown.

3.2.2 Mean Baseline Distribution

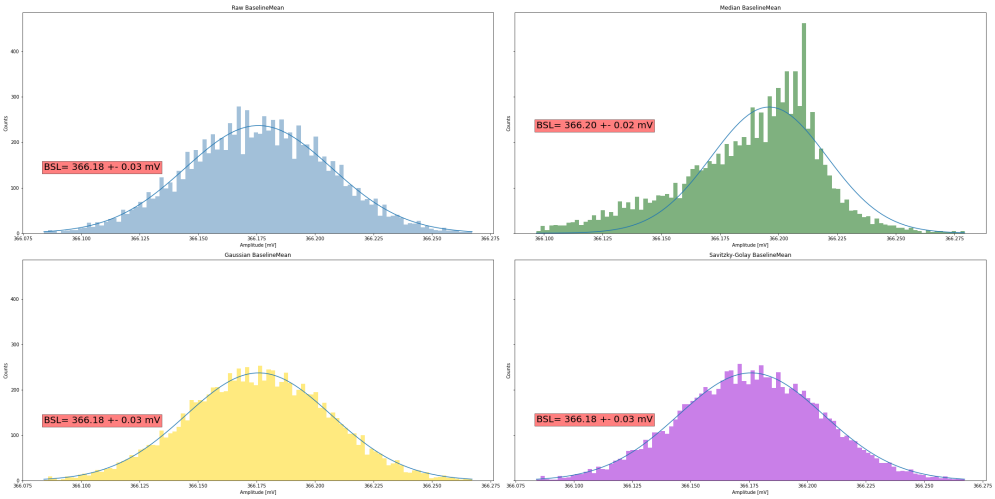

Figure 3.8: Distributions of baseline averages for all events and filters applied. Notice that the mean is the same within errors.

3.2.3 Finger Plot

Using amplitudes

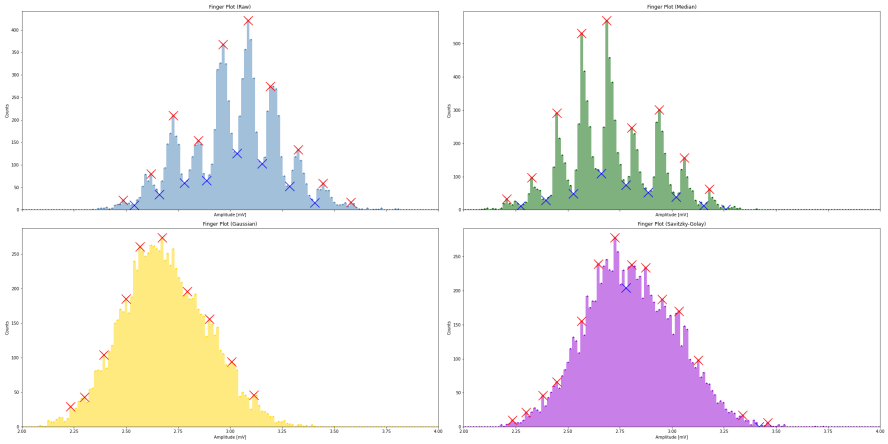

(a)

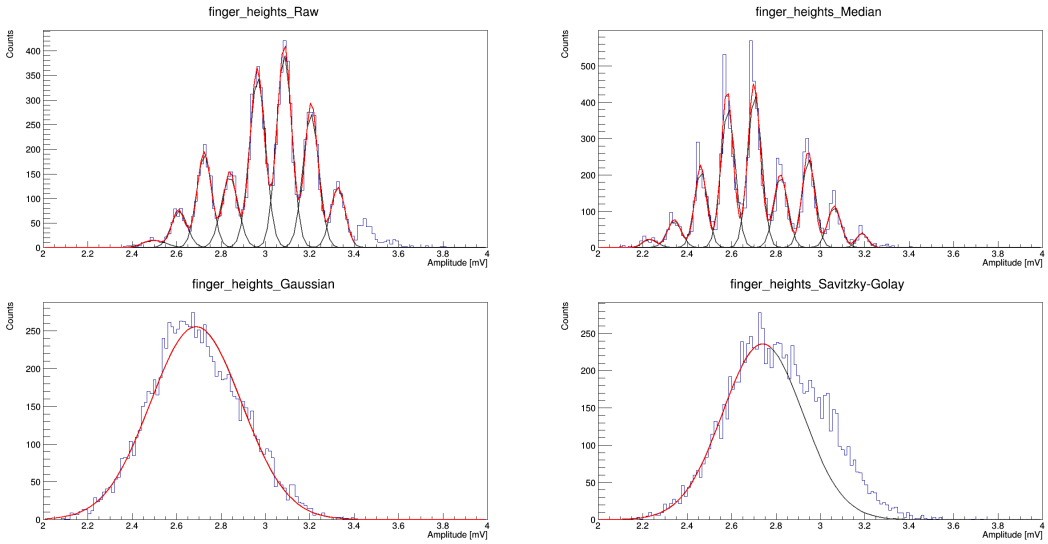

(b)

Figure 3.9: Finger Plot with peaks' amplitudes. Due to high LED intensity, the amplitudes start with high values (can't see SPE). With Gaussian and Savitzky-Golay filters there is no resolution.

Using charges

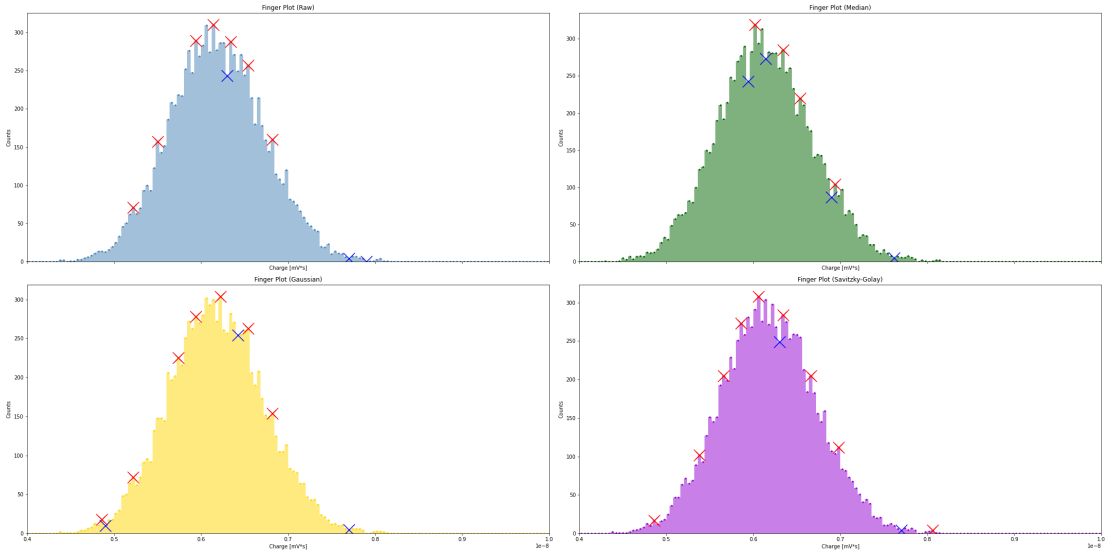

Figure 3.10: Finger Plot with peaks' charges. One can notice that there is a problem with charge, since there is no resolution (with both raw and filtered data). This behaviour needs to be futher analyzed and inspected in order to understand the reasons behind it and how to fix it. Probably, it is due to some optical noise introduced by the new analog optical transmitter.

3.2.4 Amplitude vs Time of peaks

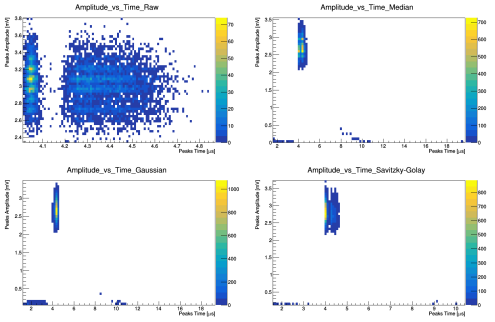

(a)

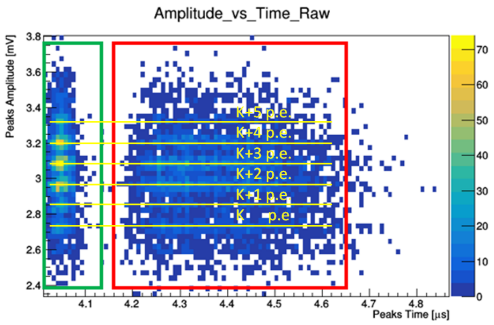

(b)

Figure 3.11: We see probably a signal region and a noise region, but further analysis are required to convalidate. Moreover, a sequence of stripes is clear, showing a descrete increase in the valuse of amplitudes, which we can impute to the arrival of a discrete number of p.e..

Chapter 4

Conclusions

4.1 Summary

In these two months being at Fermilab, I have been involved in the following tasks:

1. preparing the experimental setup shown before;
2. testing all the electrical and optical components;
3. acquiring several sets of data, changing SiPM board and Analog to Optical Transmitter;
4. data analysis, creating a code able to:
   - read all events (waveforms), plot them and apply 3 digital filters (high-frequency noise);
   - calculate and subtract baseline;
   - creating a first simple algorithm able to find peaks, integrate the in a fixed or moving window and save their main properties (amplitude, sample, time, charge);
   - plot and fit Finger Plot (using both amplitudes and charges); calculate gain (using both amplitudes and charges).

4.2 Future Plan

As future plan, I would like to:

1. take data which are usable to calculate SNR (Signal to Noise Ratio) and Resolution to SPE;
2. compare several types of SiPMs, coming from different vendors, and Analog readout boards in different configurations;
3. further improve algorithm to find peaks and integrate Finger Plots;
4. further improve code to select and discard noise and background events;
5. calculate PDE (Photon Detection Efficiency).

Appendix A

Appendix

A.1 Schematics

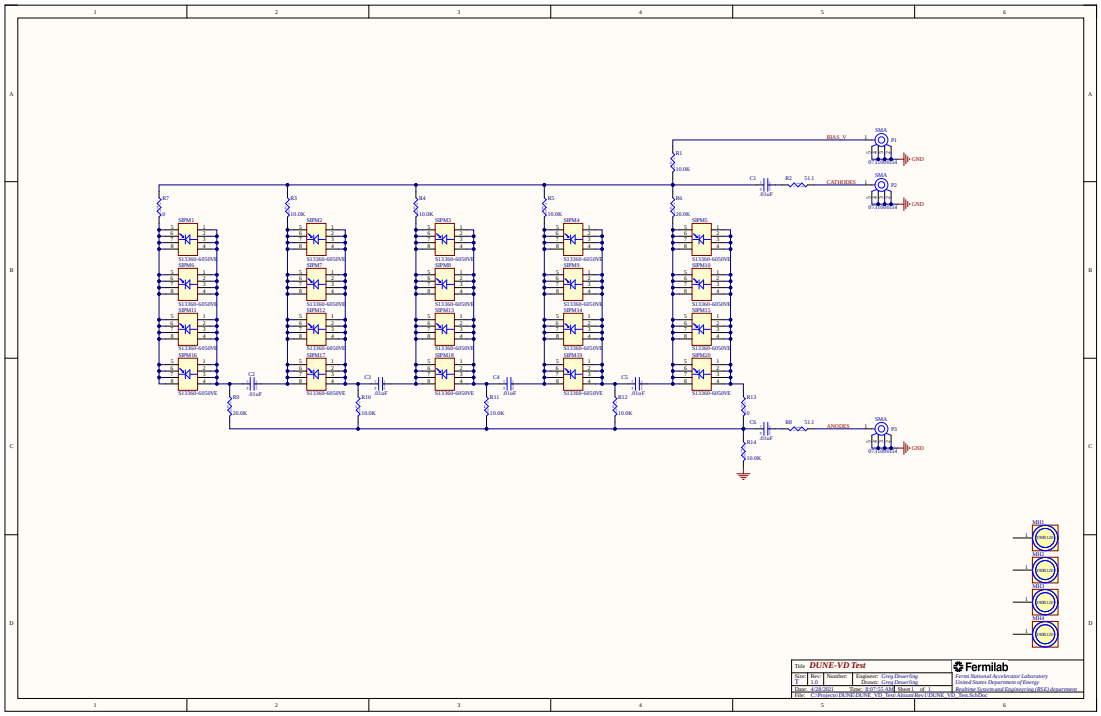

Figure A.1: Hamamatsu and Broadcom SiPM boards schematic.

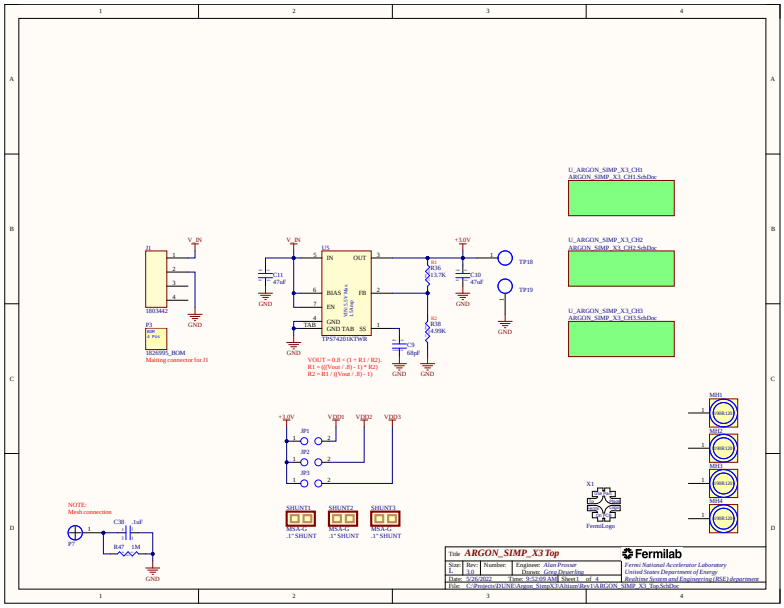

Figure A.2: Argon SimpX3 schematic.

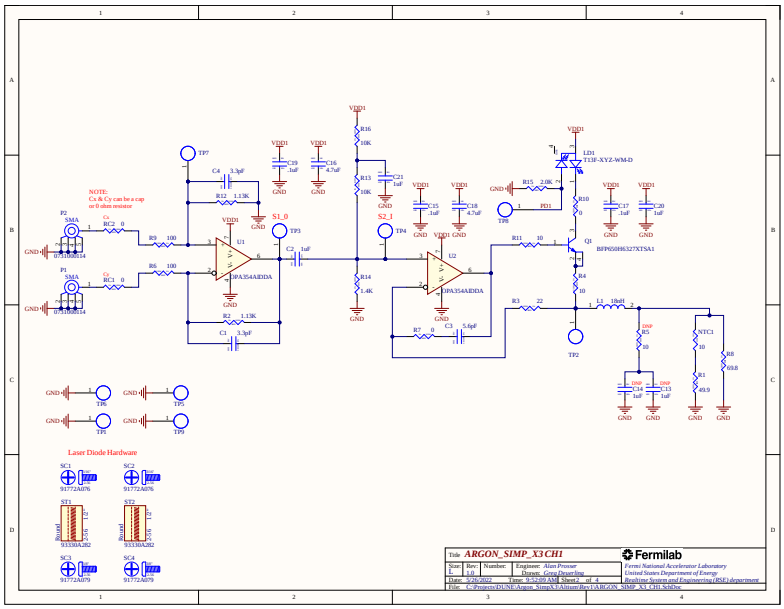

Figure A.3: Argon SimpX3 schematic.

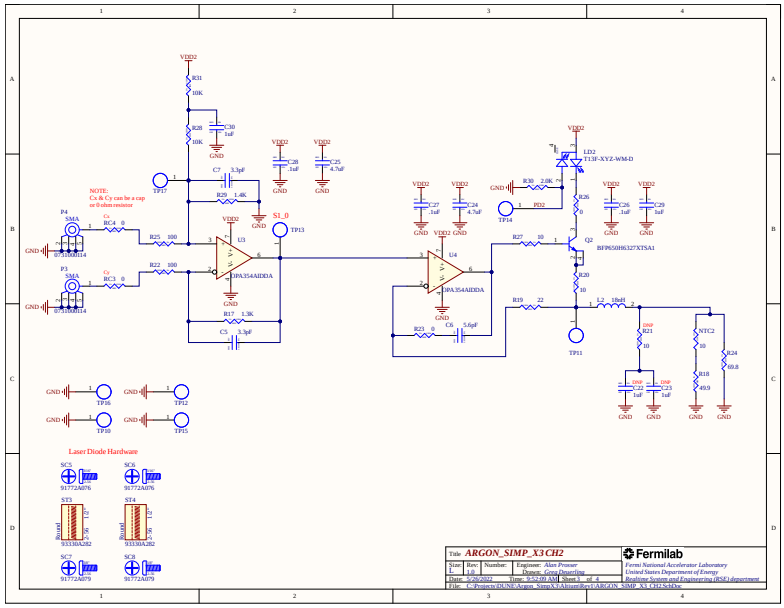

Figure A.4: Argon SimpX3 schematic.

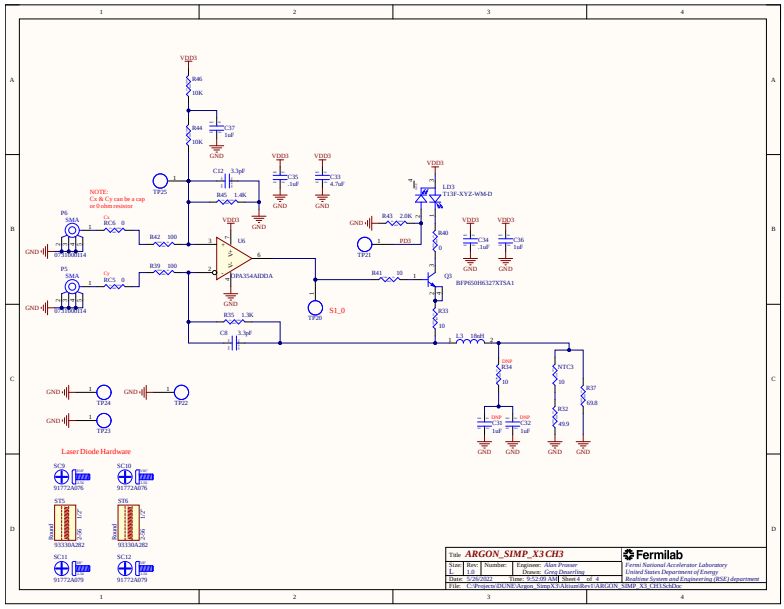

Figure A.5: Argon SimpX3 schematic.